

Accelerating the emission properties beyond the skidding effect of varying Sr, Eu and Dy concentration in SrAl₂O₄ : Eu Dy phosphors

N. Tyagi^a, D. S. Jo^a, K. Toda^b, T. Masaki^a and D. H. Yoon^{a,c,*}

^aSchool of Advanced Materials Science & Engineering, Sungkyunkwan University, Suwon 440-746, Korea

^bCenter for Transdisciplinary Research, Graduate School of Science and Technology, Niigata University, Ikarashi 2 nocho 8050, Niigata 950-2181, Japan

^cSKKU Advanced Institute of Nanotechnology (SAINT), Sungkyunkwan University, Suwon 440-746, Korea

Eu and Dy-doped strontium aluminate is a long-lasting phosphor for practical applications in displays and emergency signage. SrAl₂O₄ synthesized samples have been systematically investigated by PXRD, SEM and photoluminescence. The optimization of the properties has been determined in terms of varying concentrations of Sr²⁺ (alkali metal ion concentration) and the dopant concentrations of Eu²⁺ and Dy³⁺. A new method of synthesis requiring hydrate solutions of the metal ions and cellulose precursor called Liquid Phase Precursor method (LPP) has been adapted. The emission intensity was observed to be higher for the prepared samples compared to a commercial product prepared with a solid state reaction method.

Key words: Emission properties, PXRD, SEM, Dopant concentration, Persistent luminescence.

Introduction

In sensing applications such as bioimaging, persistent luminescent particles have found new applications apart from their unusual usage as photostimulated storage phosphors for optical information write-in and read-out processes on imaging plates [1]

Materials persistent luminescence properties with a persistence time of more than 5 h upon stimulated radiation are of fundamental interest in applications such as signage, blackouts, emergency rescue, guidance systems, and luminous watches [2-6].

Spectrum fingerprint anti-counterfeiting fiber applications are made of rare-earth strontium aluminates, which have stable physical and luminescent performance [7]. Persistent luminescence is observed in strontium aluminate phosphors with an initial rapid decay upon doping with Eu³⁺ ions or upon co-doping with an activator ion. The long afterglow characteristics of the persistent phosphors are explained on the basis of trapping and detrapping mechanisms of Dy³⁺ ion trapping [8]. Persistent luminescence phosphors based on aluminates have interesting properties, such as high radiation intensity, long-lasting photoluminescence, excellent photo resistance, robustness, color purity, and radiation resistance [9]. Moreover, multiphosphor systems such as SrAl₂O₄ : Eu²⁺, Dy³⁺, Sr₄Al₁₄O₂₅ : Eu²⁺, Dy³⁺, CaAl₂O₄ : Eu²⁺, Nd³⁺, CaSi₂O₂N₂, or Sr₂Al₆O₁₁ : Eu²⁺ and

Sr₃Al₂O₅Cl₂ lattices were prepared by spray pyrolysis, microemulsion method, and solid-state synthesis [10-15]. Other advantageous processes reported for the synthesis of SrAl₂O₄ are sol-gel synthesis, combustion synthesis, and chemical co-precipitation method [16-18].

Persistent phosphorescence or afterglow depends upon the mechanism of photooxidation of Eu²⁺ cations under UV irradiation. When an energetic beam is incident on a phosphor, an electron-hole pair diffuses through the phosphor and transfers its energy to activator ions, which subsequently results in the emission of light. The thermal energy formally releases electrons and holes trapped in defects, and their recombination occurs at radiative emission centers. For rare-earth Eu²⁺-activated phosphors, there are two types of localized centers: C and D types [19]. The type C features Eu²⁺ ions that are photo-ionized by vacuum-ultraviolet excitation and change to Eu³⁺, for which photoconductivity resulting from electrons is observed. The second is type D, in which the excitation of Eu²⁺ by ultraviolet light leads to the liberation of holes to the valence band accompanied by the reduction of Eu²⁺ to Eu¹⁺. The holes generate afterglow phosphorescence properties. In a given host, the emission of Eu²⁺ is influenced by the covalency, the size of the cation, the strength of the crystal field, and the alignment.

SrAl₂O₄ phosphor has been prepared by cellulose-assisted liquid phase precursor method using hydrate solutions of the raw materials impregnated on to the cellulose precursor. This method is apt for reducing the synthesis cost, controlling the shape and size, and creating fair crystallinity and high homogeneity for the synthesis of SrAl₂O₄ products. Strontium aluminates doped with

*Corresponding author:
Tel : +82-31-290-7388
Fax: +82-31-290-7371
E-mail: dhyoon@skku.edu

Eu²⁺ and Dy³⁺ with highly emissive properties and long afterglow have been studied.

Experimental

We used Sr(NO₃)₂ (50 wt%, Japan), Al(NO₃)₃ · 9H₂O (80 wt%, Samchun Chemical, Korea), DyCl₃ · 3H₂O (30 wt%, Japan), and EuCl₃ · 3H₂O (30 wt%, Japan) as raw materials for the synthesis of SrAl₂O₄ phosphors. The raw materials were all dissolved in deionized water to prepare their hydrate solutions and stirred thoroughly to create better homogeneity. The homogeneous hydrate solutions were then impregnated onto cellulose pulp (C₆H₁₀O₅)_n (lint-free cellulose paper, 49-μm thick, 100% cellulose, Nihun pulp, Japan) at a weight ratio of 1 : 1. The impregnated cellulose pulp was placed in an alumina crucible, rapidly fired at 600 °C for 2 h and then at 800 °C for 2 h, and finally fired at 1100 °C for 2 h in a reducing atmosphere (5H₂/95N₂). The cellulose degrades towards 400 °C and allows for the early stages of crystallization of the SrAl₂O₄ phase.

The phase purity of the products was determined by examining the powder X-ray diffraction patterns on a Rigaku X-Ray diffractometer using Cu Kα radiation (λ = 1.5418 Å) over the 2θ range of 10–80°. The SEM micrographs of products were obtained using a field emission scanning electron microscope (FE-SEM; XL-30, Philips). The fluorescence spectra were recorded at room temperature using a spectrofluorimeter (PLE/PL Drasa Pro 5300, Korea) with a xenon lamp light source.

Results and Discussion

All the samples were prepared by liquid phase precursor method and characterized by powder X-ray diffraction for structural iteration and found to form homogeneous single-phasic strontium aluminates according to JCPDS card no. 10740794. The powder X-ray diffraction pattern

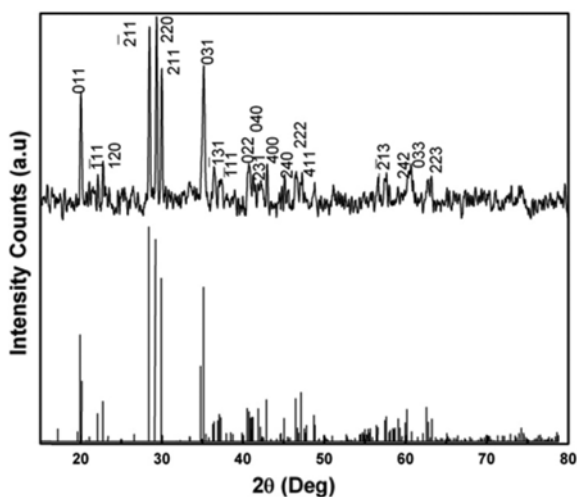


Fig. 1. The powder X-ray diffraction pattern of Sr_{1.6}Al₂O₄ : Eu_{0.015}Dy_{0.03}.

of Sr_{1.6}Al₂O₄ : Eu_{0.015}Dy_{0.03} is shown in figure 1. The structure of the low-temperature monoclinic phase of SrAl₂O₄ is represented by the 011, 020, 111, 120, 111, 211, 220, 211, 002, 031, and 131 reflections with a P2₁ space group and lattice parameters of a = 8.44 Å, b = 8.81 Å, c = 5.16 Å, and β = 93.42°. The monoclinic structure is supported by the corner sharing AlO₄ tetrahedra. The Sr ions are located in two different crystallographic sites that differ only by slight distortion of their square planes and invariably occur in channels of the tetrahedron [20]. The composition change induced no phase transformation. Additional composition data is available in Table 1. Figure 2(i) shows the scanning electron microscopic image of the synthesized SrAl₂O₄ nanophosphors and a commercial sample. In SEM,

Table 1. Compositions of Sr_xAl₂O₄ : Eu²⁺, Dy³⁺ phosphors synthesized by the LPP method.

S.No	Composition				
	Sr (mol)	Al (mol)	Eu (mol)	Dy (mol)	O (mol)
1.	1.5	2	0.015	0.03	4
2.	1.6	2	0.015	0.03	4
3.	1.7	2	0.015	0.03	4
4.	1.7	2	0.025	0.03	4
5.	1.7	2	0.035	0.03	4
6.	1.6	2	0.04	0.05	4
7.	1.6	2	0.04	0.07	4
8.	1.6	2	0.04	0.10	4
comm	0.97	2	0.01	0.02	4

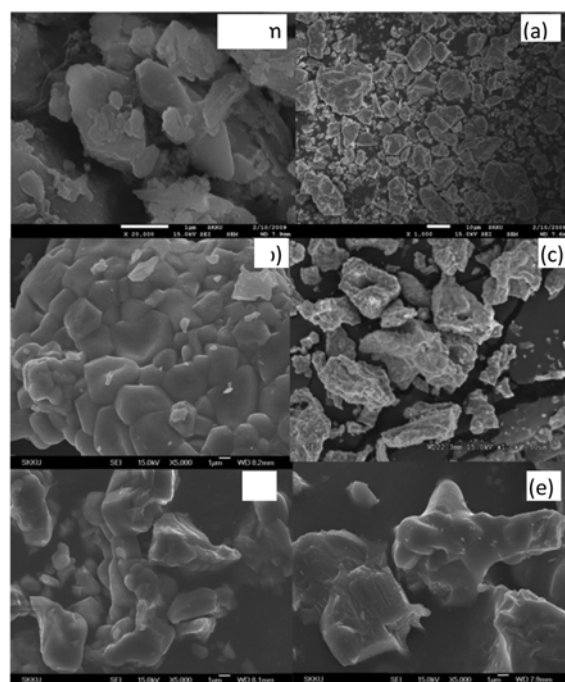


Fig. 2(i). Scanning electron microscopic images of samples a-e for compositions 2, 3, 5, 6, 8 respectively and commercial Sr_{0.97}Al₂O₄ : Eu_{0.010}Dy_{0.02}.

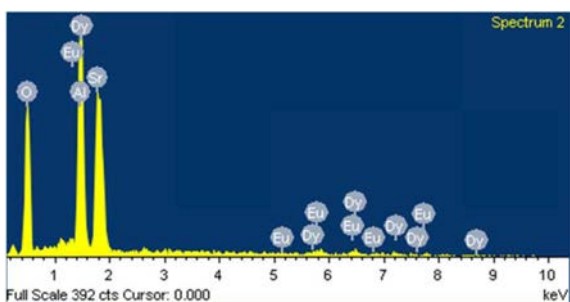


Fig. 2(ii). EDS spectrum for $\text{Sr}_{1.7}\text{Al}_2\text{O}_4 : \text{Eu}_{0.015}\text{Dy}_{0.03}$.

irregular bulky crystallites were observed with agglomeration. The SEM images do not provide insight into the compositional effect on the morphology due to heavy agglomeration. The EDS spectrum shown in Figure 2(ii) reveals agglomerates of the constitutive elements Sr, Al, O, Eu and Dy, characterizing the composition as $\text{SrAl}_2\text{O}_4 : \text{Eu}^{2+} \text{Dy}^{3+}$. This research was proposed to explain the effect of composition changes on the luminescent properties in $\text{SrAl}_2\text{O}_4 : \text{Eu}$, Dy phosphors. All the compositions are listed in Table 1. We probed the effect of varying the composition of either the host lattice by varying the Sr concentration or by altering the dopant or the auxiliary ion content, and on the basis of studying the emission or the excitation spectra. As depicted in the SEM images, the powder samples showed heterogeneity, which resulted in the determined luminescence properties.

Concentration dependence of Eu on emission properties of $\text{SrAl}_2\text{O}_4 : \text{Eu}$, Dy

The emission spectra for commercial and $\text{Sr}_{1.7}\text{Al}_2\text{O}_4 : \text{Eu}_x\text{Dy}_{0.03}$ is shown in Figure 3. A gradual increase in the emission intensity was observed as the Eu concentration was increased from 0.015 to 0.035 moles in $\text{Sr}_{1.7}\text{Al}_2\text{O}_4 : \text{Eu}_x\text{Dy}_{0.03}$ for samples 3 to 5, as shown in Table 1. The characteristic green emission at

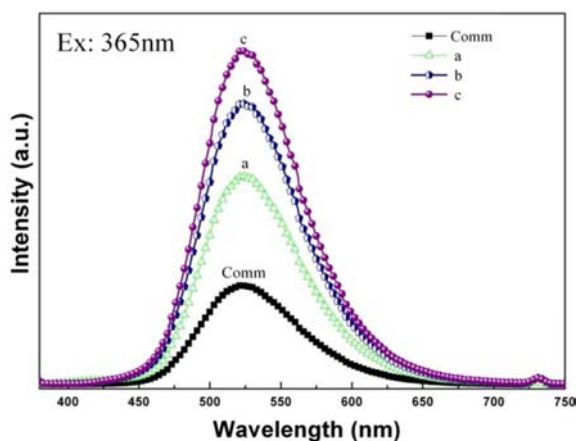


Fig. 3. The room-temperature emission spectra at $\lambda_{\text{ex}} = 365$ nm of samples; (a) = 3, (b) = 4, (c) = 5 with varying Eu concentration in $\text{Sr}_{1.7}\text{Al}_2\text{O}_4 : \text{Eu} \text{Dy}_{0.03}$ and commercial sample $\text{Sr}_{0.97}\text{Al}_2\text{O}_4 : \text{Eu}_{0.010}\text{Dy}_{0.02}$.

525 nm corresponds to the $4f^65d \rightarrow 4f^7$ transition of Eu^{2+} . The ionic radii of Eu^{2+} is 0.117 nm in O_h , and that of Sr^{2+} is 0.116 nm in O_h , so it is easily replaced by the Sr^{2+} ion in the host lattice, and the emission originates from the excited $4f^6 5d^1$ configuration of Eu^{2+} . The firing in reducing atmosphere is expected to form mainly Eu^{2+} [21]. The Eu^{2+} ions are present in two crystallographically different Sr^{2+} sites with similar environments. The emission maximum observed in the samples prepared by LPP is higher than that observed for the commercial sample. In this study, the concentration was chosen to be optimum for the activator and auxiliary ions while bearing in mind the commercial sample for the emission as well as persistent luminescence. We did not observe any transition at 450 nm, as the band is observed to disappear at higher Eu^{2+} concentration [22]. Our samples prepared by the liquid phase precursor method are shown to have better emissive properties than the commercial product prepared by solid-state method. The sample hydrate solutions impregnated on cellulose after firing yield enhanced emissive properties. The excitation profiles of these are shown in Figure 4, where we observed a broad band at 350 nm for the commercial sample with a small shoulder. Similar spectral features were observed for the prepared samples, but with a red shift ascribed to the synthesis methodology.

Concentration dependence of Dy^{3+}

We observed an increase in the emission intensity due to the increase in Dy^{3+} ion concentration while keeping other concentrations constant, as shown in Figure 5. A subtle increase in Dy^{3+} ion concentration with a mole % of 0.010 for composition 8, results in a significant increase in the emission intensity of the sample. To exhibit afterglow, it is essential for a long-lasting phosphor to have trapping levels located at suitable depth on order with the thermal release rate at

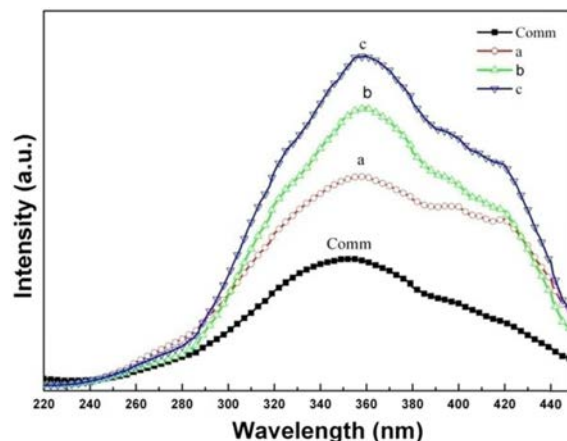


Fig. 4. The room-temperature excitation spectra at $\lambda_{\text{ex}} = 525$ nm of samples: (a) = 3, (b) = 4, (c) = 5 with varying Eu concentration in $\text{Sr}_{1.7}\text{Al}_2\text{O}_4 : \text{Eu} \text{Dy}_{0.03}$ and commercial sample $\text{Sr}_{0.97}\text{Al}_2\text{O}_4 : \text{Eu}_{0.010}\text{Dy}_{0.02}$.

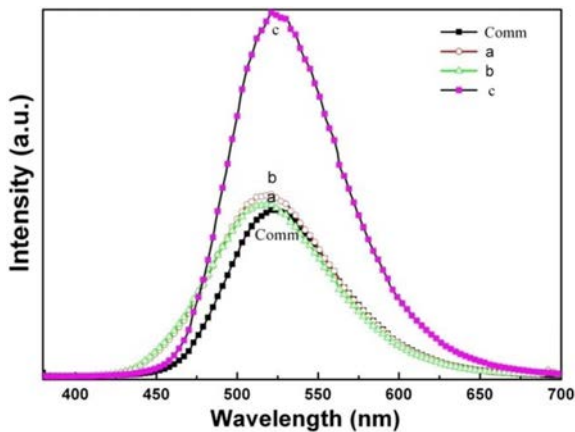


Fig. 5. The room-temperature emission spectra at $\lambda_{\text{ex}} = 365$ nm of samples: (a) = 6, (b) = 7, (c) = 8 with varying Dy concentration in $\text{Sr}_{1.6}\text{Al}_2\text{O}_4 : \text{Eu}_{0.04}\text{Dy}$ and commercial sample $\text{Sr}_{0.97}\text{Al}_2\text{O}_4 : \text{Eu}_{0.010}\text{Dy}_{0.02}$.

room temperature. The lifetime of a trapped charge carrier is given as $E_T/k_B T$, which is the ratio of trap depth to the thermal energy. To explain the charge neutrality, we propose that SrAl_2O_4 , which has Sr and oxygen vacancies, enhances the cation deficiency when it is codoped with Dy^{3+} [23]. Dy serves to increase the number and depth of electron traps. The ionization potential of the cation affects the ability of the cation to stabilize the V_o . The lower the ionization potential of the cation (Eu^{2+} 25.0eV, Dy^{2+} 41.5eV, Sr^{2+} 43.7eV), the more strongly it is attracted to the V_o . Dy^{3+} extends the phosphorescence by completing the change of V_o to electron traps by the Eu^{2+} cation attraction [23]. The excitation spectra observed for the varying Dy concentration showed dissimilar results compared to the results of samples with varied Eu content and those of the commercial sample. Instead of a peak maximum of excitation at 350 nm, it was observed at 420 nm, and only a small shoulder was present at 350 nm.

Concentration dependence of Sr^{2+}

The emission intensity does not vary monotonically with the activator Eu^{2+} ion, but depends upon the change in Sr^{2+} ion concentration. Yuan et al. studied the effect of Sr concentration in $\text{Sr}_4\text{Al}_{14}\text{O}_{25} : \text{Eu}^{2+}, \text{Dy}^{3+}$ phosphors on the luminescence properties and observed that Sr-rich phosphors have poorer afterglow properties than Al-rich phosphors [24]. But for the liquid-phase-prepared SrAl_2O_4 phosphors, we observed that the effect is different from those of the samples prepared by solid-state method. We observed enhanced emission intensity for the Sr-rich phosphors in SrAl_2O_4 phosphors, as shown in figure 5.

Conclusions

By varying the compositions, the effect of variation has been studied in SrAl_2O_4 phosphors codoped with

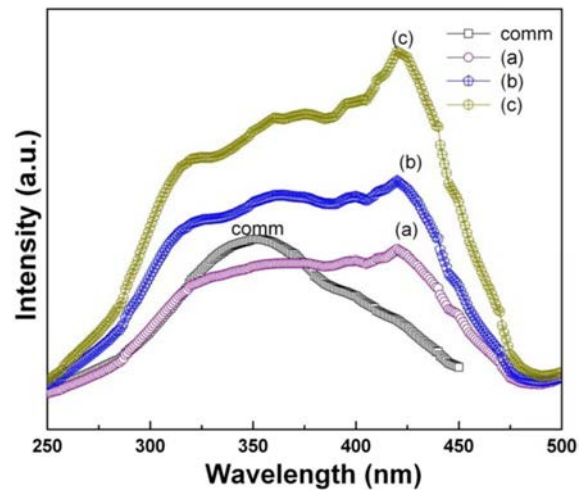


Fig. 6. The room-temperature excitation spectra at $\lambda_{\text{em}} = 525$ nm of samples: (a) = 6, (b) = 7, (c) = 8 with varying Dy concentration in $\text{Sr}_{1.6}\text{Al}_2\text{O}_4 : \text{Eu}_{0.04}\text{Dy}$ and commercial sample $\text{Sr}_{0.97}\text{Al}_2\text{O}_4 : \text{Eu}_{0.010}\text{Dy}_{0.02}$.

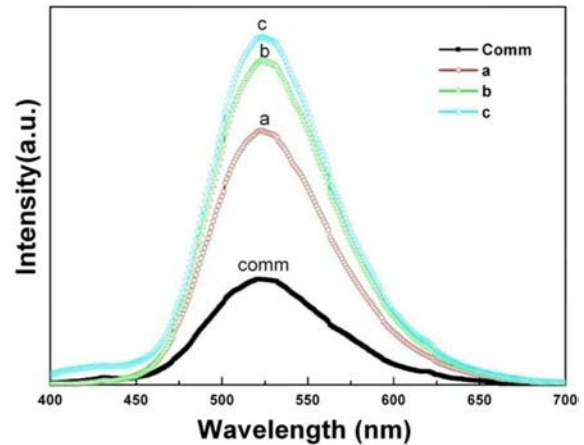


Fig. 7. The room-temperature emission spectra at $\lambda_{\text{ex}} = 365$ nm of samples: (a) = 1, (b) = 2, (c) = 3 in $\text{SrAl}_2\text{O}_4 : \text{Eu}_{0.015}\text{Dy}_{0.03}$ and commercial sample $\text{Sr}_{0.97}\text{Al}_2\text{O}_4 : \text{Eu}_{0.010}\text{Dy}_{0.02}$.

Eu and Dy using a liquid phase precursor synthesis method. The luminescence properties show a peak maximum that is higher in the prepared samples compared to the commercial product prepared with a solid-state reaction method. The characteristic green emission observed has been interpreted by studying the substitution of varying activator ions. The emission intensity was found to be significantly increased. Our analysis indicates that the effect of varying Dy content resulted in different excitation behaviors from those observed for the Eu ion composition effect. However, the emission spectra were observed to be similar in the two ascribed measurements.

Acknowledgments

This research was supported by Basic Science Research Program through the National Research Foundation of Korea (NRF) funded by the Ministry of

Education, Science and Technology (NRF-2013R1A 2A 2A01010027).

References

1. F. Liu, W. Yan, Y. J. Chuang, Z. Zhen, J. Xie and Z. Pan, *Sci. Rep.* 3 (2013) 1554.
2. W. M. Yen, S. Shionoya, H. Yamamoto, *Phosphor Handbook* (CRC Press, 2007).
3. Z. Pan, Yi-Ying Lu, Feng Liu, *Nat Mat.* 11 (2011) 58-63.
4. T. Aitasalo, P. Deren, J. Holsa, H. Jungner, J.C. Krupa, M. Lastusaari, J. Legendziewicz, J. Niittykoski, W. Streck, *J. Solid State Chem.* 171 (2003) 114-122.
5. T. Aitasalo, J. Holsa, J. C. Krupa, M. Lastusaari, J. Niittykoski, *Physics of Laser Crystals*, Kluwer Academic Publishers, Netherlands, 2003.
6. S. H. Choi, N. H. Kim, Y. H. Yun, S. C. Choi, *J. Ceram. Process. Res.* 7 (2006) 62-65.
7. J. Zhang, M. Ge, *J. Lumin.* 131 (2011) 1765-1769.
8. H. Yamamoto, T. Matsuzawa, *J. Lumin.* 72 (1997) 287-289.
9. L. Liu, Z. Zhang, L. Zhang, Y. Zhai, *Forensic Sci. Int.* 183 (2009) 45-49.
10. C. Li, Y. Imai, Y. Adachi, H. Yamada, K. Nishikubo, C. N. Xu, *J. Am. Ceram. Soc.* 90 (2007) 2273-2275.
11. C. C. Chang, C. Y. Yang, C. H. Lu *J Mater Sci: Mater Electron.* 24 2013 1450-1458.
12. Y. Wang, Lei Wang, *J. App. Phy.* 101, 2007, 053108-053105.
13. X. Song, R. Fu, S. Agathopoulos, H. He, X. Zhao, S. Zhang, *J. Applied Phy.* 106, 2009, 033103-033105.
14. H. H. Song, W. F. Liu, *Rare Metal Mat Eng.* 37, 2008, 1167.
15. D. Dutczaka, C. Ronda, A. Meijerink, T. Jüstel, *J. Lumin.* 132, 2012, 2398-2403.
16. T. Peng, L. Huajun, H. Yang, C. Yan, *Mater. Chem. Phys.* 85, 2004, 68-72.
17. T. Peng, H. Yang, X. Pu, B. Hu, Z. Jiang, C. Yan, *Mater. Lett.* 58, 2004, 352-356.
18. S. H. Choi, N. H. Kim, Y. H. Yun, S. C. Choi, *J. Ceram. Process. Res* 7, 2006, 62-65.
19. T. Matsuzawa, Y. Aoki, N. Takeuchi, Y. Maruyama, *J. Electrochem. Soc.* 143, 1996, 2670-2673.
20. M. L. Stanciu, M. G. Ciresan, N. M. Avram, *Acta Phys. Pol.* 116, 2009, 544-546.
21. M. Marchal, P. Escribano, J. B. Carda, E. Cordoncillo, *J. Sol Gel Sci. Tech.* 26, 2003, 989-992.
22. C. Beauger, Thesis, Universite de Nice, Nice, France, 1999.
23. F. Clabau, X. Rocquefelte, S. Jobic, P. Deniard, M. H. Whangbo, A. Garcia, T. L. Mercier. *Chem.* 17, 2005, 3904-3912.
24. Z. X. Yuan, C. K. Chang, D. L. Mao, W. J. Ying, *J. Alloys Compd.* 377, 2004, 268-271.